Effects of water and fines contents on the resilient modulus of the interlayer soil of railway substructure

Trong Vinh Duong, Yu-Jun Cui, Anh Minh Tang, Jean Claude Dupla, Jean Canou, Nicolas Calon, Alain Robinet

Effects of water and fines contents on the resilient modulus of the interlayer soil of railway sub-structure

Trong Vinh DUONG, Yu-Jun CUI, Anh Minh TANG, Jean-Claude DUPLA, Jean CANOU, Nicolas CALON, Alain ROBINET

Trong Vinh DUONG
Ecole des Ponts ParisTech, Laboratoire Navier/CERMES

Yu-Jun CUI
Ecole des Ponts ParisTech, Laboratoire Navier/CERMES

Anh Minh TANG
Ecole des Ponts ParisTech, Laboratoire Navier/CERMES

Jean-Claude DUPLA
Ecole des Ponts ParisTech, Laboratoire Navier/CERMES

Jean CANOU
Ecole des Ponts ParisTech, Laboratoire Navier/CERMES

Nicolas CALON
French Railway Company (SNCF)

Alain ROBINET
French Railway Company (SNCF)

Corresponding author:
Prof. Yu-Jun CUI
Ecole des Ponts ParisTech
6-8 av. Blaise Pascal, Cité Descartes, Champs-sur-Marne
F-77455 Marne – la – Vallée cedex - France
Telephone: +33 1 64 15 35 50
Fax: +33 1 64 15 35 62
E-mail: yujun.cui@enpc.fr

Abstract

This paper deals with the resilient behavior of the interlayer soil which is created mainly by the interpenetration of ballast and sub-grade soils. The interlayer soil studied was taken from a site in the South-East of France. Large-scale cyclic triaxial tests were carried out at three water contents (w = 4, 6 and 12%) and three fines contents corresponding to 5% sub-grade added to the natural interlayer soil, 10% sub-grade added to the natural interlayer soil and 10% fine particles (< 80 μm) removed from the natural interlayer soil. Soil specimens underwent various deviator stresses, and for each deviator stress a large number of cycles were applied. The effects of deviator stress, number of cycles, water content and fines content on the resilient modulus (M_r) were analyzed. It appears that the effects of water content and fines content must be analyzed in a global fashion because the two effects are closely linked. Under unsaturated conditions, the soil containing high fines content has higher resilient modulus due to the contribution of suction. When the soil approaches the saturated state, it loses its mechanical performance with a sharp decrease in resilient modulus.

Keywords: railway sub-structure; interlayer soil; resilient modulus; fines content; water content; large-scale cyclic triaxial test.

Introduction

The soils in the sub-structures of highway and railway are subjected to a huge number of traffic loading cycles. In this context, the resilient modulus of sub-structure soils is an important parameter to be considered when designing new tracks or when maintaining under-operation tracks. Indeed, several authors [1, 4, and 28] reported that the resilient modulus of sub-grade can strongly influence the mechanical behavior of sub-structure.

For the French ancient railway tracks constructed in the 1880s, as ballast was placed directly on the sub-grade during the construction without any separation layers, an interlayer was naturally created over time mainly by the interpenetration of ballast and sub-soil under the traffic effect [5-7, 32]. This interlayer has been kept as part of the sub-structure considering its high mechanical performance related to its high unit mass [33]. As the interlayer is a "component" of the sub-structure overlying the sub-grade, its mechanical behavior appears to be of primary importance for the overall behavior of sub-structure even the overall track structure. However, because this material has been formed naturally, it can present large variability in terms of fines natures and fines contents. Moreover, under the effect of climatic conditions, soil water content changes also constantly. These changes in fines content, fines nature and water content can greatly affect soil mechanical behavior such as soil resilient modulus.

The notion of resilient behavior appeared for the first time in the middle of the 20th century [16, 17]. In the railway context, the resilient modulus (M_r) is defined as the secant slope of the curve of deviator stress versus axial strain obtained from cyclic triaxial tests [21, 26-28, 30, and 37]. Previous studies showed that there are several factors that affect the resilient modulus of unbound granular materials, in particular the stress level [14, 22, 24, 26, and 30]. The increase in moisture content appears to decrease the resilient modulus [10, 11, and 14]. For the effect of loading cycles, a large disagreement exists in terms of number of cycles required to reach the stabilization of resilient modulus [23, 24, 30, 35, 36]. As far as the effect of fines content is concerned, there is no conclusive observation as mentioned by Lekarp et al. [24]. Thom and Brown [31] and Kamal et al. [20] reported that the resilient modulus generally decreases when the fines content increases. However, Jorenby and Hicks [19] observed that the stiffness of crushed aggregate has an initially increase trend followed by a considerable reduction when clayey fines content increased.

All these factors (moisture content, fines content, number of cycles) influence the resilient response of materials. However, to the authors' knowledge, their combined effect has rarely investigated especially for the interlayer soil. In the present work, large-scale cyclic triaxial tests were carried out to study the variations of M_r of an interlayer soil under the combined effects of stress level, water content, fines content and cyclic loadings.

Materials and methods

The studied interlayer soil was taken from Sénissiat, near Lyon, France. The grain size distribution curves of the natural interlayer soil (ITL_0) and the sub-grade soil (SG) are presented in Fig. 1. It can be observed that the interlayer soil has a large fines content (16% of particles are smaller than 80 µm), and its grain size distribution curve is well graded from ballast size (60 mm) to clay size (< 2 µm). Its physical properties (density, plasticity index, blue methylene value and proctor curve) of this material were reported by Trinh et al. [33, 34]. For the SG, almost all soil particles are smaller than 80 µm.

In order to study the influence of fines content, the fines content of the soil was varied by either removing fine particles smaller than 80 µm from the interlayer soil (-10% for ITL_{-10}) or adding sub-grade soil into the interlayer soil (+5% for ITL_5 and +10% for ITL_{10}). The percentages refer to the ratio of dry mass of fine particles to dry mass of interlayer soil. The removal of fine particles for the preparation of ITL_{-10} was done by sieving. The grain size distribution curves of ITL_{-10}, ITL_5 and ITL_{10} are also shown in Fig. 1.

For the specimen preparation, water were first added and mixed with the material using a large mixer to reach the target water content. After mixing, the wet materials were stored in hermetic containers for at least 24 h for moisture homogenization. Compaction was performed in 6 layers of 0.1 m thick each using a vibratory hammer to a dry unit mass of 2.01 Mg/m^3. This is the maximum dry unit mass which can be reached in the adopted conditions without breaking ballast particles.

Because large particles were involved, a large-scale triaxial apparatus developed by Dupla et al. [8] was used, enabling specimens of 300 mm in diameter and 600 mm in height to be tested. This apparatus can apply large number of loading cycles (up to several millions) at a frequency up to several tens of Hertz.

The program of tests is presented in Table 1. All the four soils were tested at three water contents (w = 4%; 6% and 12%) corresponding to three initial degrees of saturation (S_{ri} = 32%; 49% and 100%), except ITL_5 on which only one test at a water content of w = 6% was conducted owing to lack of material. The tests are named according to the material (ITL_{-10}, ITL_0, ITL_5, ITL_{10}) and water content. For instance, ITL_0w4 corresponds to the test on ITL_0 at 4% water content. To overcome the problem related to the limited material quantity, the multi-step loading procedure proposed by Gidel et al. [12] was adopted. This procedure enables several deviator stress levels to be applied before the soil specimen reaches the failure state, thereby reducing the number of tests on one hand and avoiding the effect of variability of soil specimens on the other hand.

The cyclic triaxial tests were performed under a constant confining pressure σ_3 = 30 kPa. This value was chosen by referring to the wheel load generated by train [2], the depth of the interlayer (from 250 mm to 600 mm), the Poisson's ratio (0.3 - 0.4 as proposed by Selig and Waters [28]). The vertical stress at the top of interlayer was found to be 40 to 90 kPa. These values correspond to the Indian railways as reported by Jain and Keshav [18] and American railways as reported by Selig and Waters [28] and Yang et al. [39]. In other countries where heavier wagons are used, the wheel load may reach 30 tons per axle [2], leading to a vertical stress of 120 to 140 kPa on the interlayer [13, 18, 25]. In this study, a maximum deviator stress of 200 kPa was applied. All the tests were performed under drained condition; the valves were open (under unsaturated condition) or connected to a water back pressure source (under saturated condition). During the saturated triaxial test, the back pressure was kept constant and pore water can drain freely. For the loading frequency, a value of 5 Hz was chosen because this is the dominant one among a number of frequencies generated in the French ancient sub-structures at a train speed of 100 km/h [29]. During the tests, the deviator stress was increased in steps from 0 to various target values; in each step, 30 000 cycles were applied and the variations of axial strain were recorded.

Results

Fig. 2 presents typical curves of deviator stress versus axial strain for the first cycles in test ITL_5w6. It also shows the definition of permanent axial strain (ε_p), the resilient axial strain (ε_r) through the first cycle. It can be observed that the minimum deviator stress did not totally reach zero for all cycles. This was probably due to the high loading/unloading speed (frequency of 5 Hz) that caused a delay between the target signal and the real signal. However, it is believed that this problem does not affect the resilient modulus (M_r) that corresponds to the secant slope of curves (see Fig. 2).

Fig. 3 plots the deviator stress versus the axial strain for the moments where the values of Δq_{max} were increased: during the first 8 cycles (N = 8) under Δq_{max} = 45 kPa (Fig. 3*a*), from Δq_{max} = 45 kPa (N = 30 000) to Δq_{max} = 90 kPa (N = 30 001 - 30 0004) (Fig. 3*b*), from Δq_{max} = 90 kPa (N = 60 000) to Δq_{max} = 145 kPa (N = 60 001 - 60 0004) (Fig. 3*c*) and from Δq_{max} = 145 kPa (N = 90 000) to Δq_{max} =20 kPa (N = 90 001 - 90 0004) (Fig. 3*d*). It can be observed that when a new deviator stress was applied, the axial strain increased accordingly. During the very first cycles under each stress level, the loading and unloading paths did not form close cycles, suggesting that significant permanent axial strain developed. In this case, the resilient modulus was determined based on the unloading path of a cycle and the loading path of the next cycle. The hysteresis loop was large in the first cycles, and with the increase of number of cycles, this hysteresis became less and less significant. At large number of cycles by the end of each loading level, the material behaved almost in a purely elastic fashion. Werkmeister et al. [38] reported that the change in the loop shape provides information about the different deformation mechanisms. In the beginning, there was probably particles rotation and rearrangement producing the plastic strain. Over time, these particles movements became limited and a purely resilient state is reached where strain is due to the deformation at the contacts of particles. Note that the shape of loading/unloading loops is related to the slope adopted for the determination of the resilient modulus. When two paths formed a close cycle, the straight line between the lowest and highest point of the loading/unloading cycle was used in the determination.

Fig. 4 depicts the evolution of resilient strain with number of cycles for test ITL_2w12. When the deviator stress increased, the resilient strain increased sharply during the first cycles of each stress level, and decreased afterwards to reach stabilization. The resilient strain was larger under higher deviator stress.

Fig. 5 depicts the variations of M_r with the number of cycles (N) at three water contents and various deviators stress levels for ITL_{10}. In the case of $ITL_{10}w4$ (Fig. 5a) at Δq_{max} = 23 kPa, the data of resilient modulus shows some scatter, but in general an increase trend can be identified. Because of the data scatter, it is difficult to determine the number of cycles at which the stabilization of resilient modulus started. The values in other stress levels are more or less constant around 250 MPa. For $ITL_{10}w6$ (Fig. 5b), the resilient modulus for all stress levels are found to increase significantly in the beginning and then stabilize after around 15 000 cycles. When Δq_{max} was increased from 45 kPa to 90 kpa, the resilient modulus rose up sharply. By contrast, an opposite trend was observed when Δq_{max} was increased from 90 to 140 kPa. It can be seen from Fig. 5c that for each deviator stress level, the resilient modulus decreased during the first cycles. For instance, it decreased from 168 MPa to 144 MPa from cycle 1 to cycle 7. However, this decreasing trend came very quickly to its end and was replaced by an increasing one. Afterwards, the increase rate slowed down and the resilient modulus value tended to stabilize after about 5000 loading cycles. Referring to Fig. 4, the significant variations of resilient modulus in Fig. 5 correspond to the phase characterized by quick development of resilient axial strain just after the change of stress level, and the stabilization states of resilient modulus corresponds to the stabilization of resilient axial strain.

These observations are confirmed in the case of ITL_5w6 (see Fig. 6). For all stress levels, the resilient modulus increased with the number of cycles during the first cycles. At Δq_{max} = 45 kPa about 10 000 cycles were needed for the resilient modulus to become stable while at Δq_{max} = 140 kPa and 200 kPa, about 5000 cycles were needed. The variation range of M_r at all stress levels is about ±10 MPa. On the whole, the effect of deviator stress is not as clear as in the case of $ITL_{10}w6$.

The results of ITL_0 are presented in Fig. 7. The variation of M_r with N is more pronounced in the case of ITL_0w12 (Fig. 7c) than in the cases of ITL_0w4 (Fig. 7a) and ITL_0w6 (Fig. 7b). After the first variations when the deviator stress Δq_{max} changed, the resilient modulus increased with the number of cycles in the case of ITL_0w12, while the changes in the two other cases are not clear.

As regards ITL_{-10}, the results with three different water contents are presented in Fig. 8. In the two cases of w = 4% and 12%, the resilient modulus did not vary much for the deviator stress up to 90 kPa, suggesting an insignificant influence of the number of cycles. Also, the influence of Δq_{max} is insignificant because albeit the variation of Δq_{max}, the resilient modulus remained at a steady value: about 230 MPa for $ITL_{-10}w12$ and 250 MPa for $ITL_{-10}w4$. In the case of w = 6% (Fig. 8b), the variation is clearer as the results show a slight increasing trend of M_r with the number of cycles and Δq_{max}. At the stress level of 140 kPa, there was a sharp decrease of M_r, regardless of the water content: for the three tests, when Δq_{max} was increased from 90 kPa to 140 kPa, a reduction of M_r of about 50 kPa was produced. Afterwards, the variations of resilient modulus with the number of cycles became much more pronounced than in the cases of other deviator stress levels.

Discussions

From the test results, it was observed that after a few scattered results at the beginning of each stress level, the resilient modulus became stable with the number of cycles. However, the variations were different for different soils and different water contents. The variations were clear in the case of ITL_{10} (Fig. 5b and c), insignificant in the first part of test ITL_0w4 (Fig. 7a) and ITL_{-}

$_{10}w4$ (Fig. 8a). The stabilization value was reached right after the first cycles in test ITL_0w4 (see Fig. 7a) and after 15 000 cycles in test $ITL_{10}w6$ (see Fig. 5b). Therefore, it can be stated that the number of cycles needed for M_r to reach stabilization depends on the stress level, water content, and fines content. This can explain the disagreement found in literature regarding the number of cycles required to attain a stable resilient state: Stewart [30] studied the ballast behavior and reported a stabilization after 1000 cycles while Hicks and Monismith [14] and Allen and Thompson [3] (cited by Lekarp et al. [24] and Lackenby [23]) observed that 50 – 100 cycles are needed for the stabilization for granular materials.

The variations of resilient modulus during the scattered phase at the beginning of each Δq_{max} were observed in all tests. This phase corresponds to the stage where the permanent axial strain developed quickly and the loading/unloading path did not form a close cycle in the deviator stress – axial strain plane. This can be explained as follows: when Δq_{max} was increased, the soil behavior became elasto-plastic; thus irreversible strain was produced. However, this phenomenon occurred during the first loading. Afterwards, the cyclic loading led to a progressive stabilization of the particles arrangement, thereby a negligible plastic strain.

For a better analysis on the effects of deviator stress and water content, the end-level resilient modulus values (after 30 000 cycles for each deviator stress level) are plotted versus deviator stress in Fig. 9. For ITL_{10} (Fig. 9a), the results at 4% and 12 % water contents present a slight decrease of resilient modulus when the deviator stress was increased from 23 to 102 kPa. On the contrary, in the case of 6% water content, the resilient modulus increased and then reached stabilization. The values of 4% and 6% water contents fall in the same range, around 250 MPa and clearly higher than the values of 12% water content. For ITL_0 (Fig. 9b), at 4% and 6% water content, the resilient modulus increased with the deviator stress and the values of 4% are higher than those of 6%. The values of ITL_0 in near saturated state (w = 12%) are, as opposed to the case of ITL_{10}, higher than those of 4% water content. In the case of ITL_{-10} (Fig. 9c), the curves have almost the same shape: a stage of slight variations up to 90 kPa of deviator stress followed by a stage of decrease, the decrease being more pronounced in the case of $ITL_{-10}w12$.

In terms of water content effect, the value of ITL_{-10} at 4% water content is the highest; the values of 12% water content are lower than those of 4% water content but higher than those of 6% water content. The relative positions of these curves show that the water content effect is not the same for the three materials. It appears that the increase of water content brings a negative effect to the resilient modulus of the soil that has the highest fines content (ITL_{10}). However, for ITL_0 and ITL_{-10}, the resilient modulus decreased when water content changed from 4% to 6% but increased when water content was increased to 12%. Note that only a decreasing trend of resilient modulus with growing saturation level for granular material was observed by Lekarp [24]. More studies are required to clarify this issue.

For ITL_{-10}, a deviator stress of 90 kPa appears to be the critical value for the variations of resilient modulus: all tests showed a decrease of resilient modulus at this stress level, suggesting a significant change in soil behavior. As mentioned previously, after a certain number of cycles, the resilient behavior was mainly governed by the contacts of soil particles. When the imposed deviator stress increased, the stress applied at the inter-particles contact exceeds its limit and particle breakage may occur. As a result, a sharp decrease of M_r is produced. This could be the case for ITL_{-10} that has the lowest fines content. For ITL_0 and ITL_{10}, this phenomenon of particle breakage was probably attenuated, leading to much smaller decrease of M_r.

As far as the effect of water content is concerned, the results show that the relative positions of the curves of three different water contents are not the same for the three materials. This suggests that the soil composition can strongly influence the material resilient modulus. Fig. 10 presents the results according to the water content: 4%; 6% and 12% in Figs. a, b and c, respectively. The effect of fines content can be observed clearly. In the case of *w* = 4%, the results of ITL_{-10} and ITL_{10} are almost identical for the deviator stress up to 100 kPa. But much lower values are observed for ITL_0 for the deviator stress up to 140 kPa. Beyond 140 kPa deviator stress, the values become almost the same for ITL_{-10} and $ITL_{0.}$ At 6% water content, the resilient modulus of ITL_0 is also the smallest, showing that when decreasing the fines content (from ITL_{10} to ITL_0), a reduction of resilient modulus is produced. However, when the fines content is decreased to a level as low as ITL_{-10}, the resilient modulus starts to increase. Under the near saturation conditions (*w* = 12% in Fig. 10c), it is observed that the greater the fines content, the lower the resilient modulus.

Fig. 11 plots the end stage resilient modulus at three stress levels with the variation of water content and fines content. Despite of the scatter, it can be generally observed a clear trend of M_r at all water content. It slightly deceases when the fine content added increases from -10% to 0%. After that, it can be observed a significant increase of M_r when the fine content added passes to 10%. Adding more fine particles, in one hand, limited the contact between big particles contact (ballast), but in other hand, increase the suction, as the gravimetric water content was kept constant.

To identify the mechanisms of these phenomena, it appears necessary to consider the combined effects of the fines content and the water content which is linked to the soil suction. It is well known that for unsaturated soils, suction contributes to the soils shear strength, especially for the fine-grained soils. This explains why fine particles show a positive effect on the resilient modulus under unsaturated conditions, but a negative effect under saturated conditions. It can be observed in the case of Δq_{max} = 45 kPa (Fig. 11a), for the case of 12% of water content, there was no more suction effect, and the resilient modulus decrease with the increase of fine content. This implies that in unsaturated conditions, due to the suction effect the interlayer soil containing high fines content has a better mechanical performance, while in near saturation conditions, higher fines contents leads to a significant degradation of mechanical performance. This is in agreement with the observations of Huang et al. [15], Ebrahimi [9] and Duong et al. [7]. From a practical point of view, these findings are important for the maintenance of railway tracks. If the soil containing high fines content can satisfy the requirements in terms of resilient modulus under unsaturated conditions, measures must be taken to protect it from water infiltration. Very often, it is a good drainage system that should be set up for this purpose.

Conclusions

The resilient behavior of an interlayer soil taken in a railway sub-structure in France was studied in the laboratory. The effects of deviator stress level, number of cycles, water content and fine content were investigated by performing large-scale cyclic triaxial tests. Four fines contents and 3 water contents were considered.

At each deviator stress level, after the first scattered results due to the plastic behavior of soil, the resilient modulus tended to stabilize with the number of cycles. It was found that the number of cycles needed to reach stabilization depends on the material nature, water content and stress level.

The effects of water content and of fines content are linked, and it appeared impossible to distinguish the two effects. Indeed, in unsaturated conditions, due to the suction effect, the soil having high fines content showed higher resilient modulus. On the contrary, when the soil approached the saturated conditions, the fine particles provided a negative effect. This suggests that drainage measures must be taken to protect the interlayer soil when its mechanical performance appears satisfactory under unsaturated conditions but unsatisfactory under saturated conditions.

Acknowledgements

This study was carried out within the research project RUFEX “Reuse and reinforcement of ancient railway sub-structure and existing foundations”. The authors would like to address their deep thanks to Ecole des Ponts ParisTech (ENPC), Railway Network of France (RFF), French Railways Company (SNCF) and French National Research Agency for their supports.

References

1. ASSHTO (1993) Guide for design of pavement structures.

2. Alias J (1984) La voie ferrée. Techniques de construction et d'entretien. 2nd Ed., Eyrolles (In French).

3. Allen JJ, Thompson MR (1974) Resilient response of granular materials subjected to time dependent lateral stresses. Transportation Research Record 510:1-13.

4. Basudhar PK, Ghosh P, Dey A, Valsa S, Nainegali LS (2010) Reinforced earth design of embankment and cuts in railway. Research Designs and Standards Organization, Department of Civil Engineering, Indian Institute of Technology Kanpur.

5. Cui YJ, Duong TV, Tang AM, Dupla J, Calon N, Robinet A (2013) Investigation of the hydro-mechanical behaviour of fouled ballast. Journal of Zhejiang University- Science A, 14(4):244-255.

6. Duong TV, Trinh VN, Cui YJ, Tang AM, Calon N (2013*a*) Development of a large-scale infiltration column for studying the hydraulic conductivity of unsaturated fouled ballast. Geotechnical Testing Journal 36(1):1-10.

7. Duong TV, Tang AM, Cui YJ, Trinh VN, Dupla JC, Calon N, Canou J, Robinet A (2013*b*) Effects of fines and water contents on the mechanical behavior of interlayer soil in ancient railway sub-structure. Soils and Foundations (accepted for publications).

8. Dupla JC, Pedro LS, Canou J, Dormieux L (2007) Mechanical behaviour of coarse grained soils reference. Bulletin de Liaison des Laboratoires des Ponts et Chaussées (268-269):31-58.

9. Ebrahimi A (2011) Behavior or fouled ballast. Railway Track and Structures 107(8):25–31.

10. Ekblad J, Isacsson U (2008) Influence of water and mica content on resilient properties of coarse granular materials. International Journal of Pavement Engineering 9(3):215–227.

11. Ekblad J (2007) Influence of water on coarse granular road materials properties. PhD dissertation, Royal Institute of Technology KTH, Stockholm, Sweden.

12. Gidel G, Hornych P, Chauvin JJ, Breysse D, Denis A (2011) A new approach for investigating the permanent deformation behavior of unbound granular material using the repeated load triaxial apparatus. Bulletin de Liaison des Laboratoires des Ponts et Chaussées 233:5-21.

13. Grabe P, Clayton C (2009) Effects of principal stress rotation on permanent deformation in rail track foundations. Journal of Geotechnical and Geoenvironmental Engineering 135(4):555–565.

14. Hicks RG, Monismith CL (1971) Factors influencing the resilient response of granular materials. Highway Research Record 345:15–31.

15. Huang H, Tutumluer E, Dombrow W (2009) Laboratory characterization of fouled railroad ballast behavior. Journal of the Transportation Research Board 2117(1):93–101. http://dx.doi.org/10.3141/2117-12.

16. Hveem FN (1955). Pavement deflections and fatigue failures. In Highway research board bulletin, Highway Research Board 114:43–87.

17. Hveem FN, Carmany RM (1948) The factors underlying the rational design of pavements. In Highway Research Board Proceedings 28:101–136.

18. Jain V, Keshav K (1999) Stress distribution in railway formation–a simulated study. Proceeding of the 2nd International Symposium on Pre-Failure Deformation Characteristics of Geomaterials–IS Torino pp. 653–658.

19. Jorenby BN, Hicks RG (1986) Base course contamination limits. Transportation Research Record 1095, Transportation Research Board, Washington, D.C. pp.86–101.

20. Kamal MA, Dawson AR, Farouki OT, Hughes DAB, Sha'at AA (1993) Field and laboratory evaluation of the mechanical behaviour of unbound granular materials in pavements. Transportation Research Record 1406, Transportation Research Board, Washington, D.C. pp. 88–97.

21. Kim D, Kim JR (2007) Resilient behavior of compacted subgrade soils under the repeated triaxial test. Construction and Building Materials 21(7):1470–1479.

22. Kolisoja P (1997) Resilient Deformation Characteristics of Granular Materials. PhD dissertation, Tampere University of Technology, Finland.

23. Lackenby J (2006) Triaxial behaviour of ballast and the role of confining pressure under cyclic loading. PhD dissertation, University of Wollongong.

24. Lekarp F, Isacsson U, Dawson A (2000) State of the art. I: Resilient response of unbound aggregates. Journal of transportation engineering 126(1):66–75.

25. Li D, Selig E (1998) Method for railroad track foundation design. I. Development. Journal of Geotechnical and Geoenvironmental Engineering 124(4):316–322.

26. Lim WL (2004) Mechanics of railway ballast behaviour. PhD dissertation, University of Nottingham.

27. Radampola S (2006) Evaluation and modelling performance of capping layer in rail track substructure. Thesis dissertation, Central Queensland University.

28. Selig ET, Waters JM (1994) Track geotechnology and substructure management. Thomas Telford.

29. SNCF (2009) R2520-2009-01 - Sollicitations mécaniques dans la plate-forme: Mesures d'accélérations verticales dans la plate-forme. Technical report (In French).

30. Stewart HE (1982) The prediction of track performance under dynamic traffic loading. PhD Dissertation, University of Massachusetts.

31. Thom NH, Brown SF (1987) Effect of moisture on the structural performance of a crushed-limestone road base. Transportation Research Record 1121, Transportation Research Board, Washington, D.C. pp. 50–56.

32. Trinh VN (2011) Comportement hydromécanique des matériaux constitutifs de plateformes ferroviaires anciennes. PhD Dissertation, Ecole Nationales des Ponts et Chaussées - Université Paris – Est, France (In French).

33. Trinh VN, Tang AM, Cui YJ, Canou J, Dupla J, Calon N, Lambert L, Robinet A, Schoen O (2011) Caractérisation des matériaux constitutifs de plate-forme ferroviaire ancienne. Revue Française de Géotechnique (134-135): 65–74 (In French).

34. Trinh VN, Tang AM, Cui YJ, Canou J, Dupla J, Calon N, Lambert L, Robinet A, Schoen O (2012) Mechanical characterisation of the fouled ballast in ancient railway track sub-structure by large-scale triaxial tests. Soils and Foundations 52(3):511-523.

35. Uthus L, Hoff I, Horvli I (2005) A study on the influence of water and fines on the deformation properties of unbound aggregates. In Proceedings, 7th Internacional Conference on the Bearing Capacity of Roads, Railways and Airfields, Trondheim, Norway.

36. Uthus L (2007) Deformation Properties of Unbound Granular Aggregate. PhD dissertation, Norwegian University of Science and Technology.

37. Werkmeister S (2003) Permanent deformation behaviour of unbound granular materials in pavement constructions. Thesis dissertation, Fakultät Bauingenieurweser der Technischen Universität Dresden.

38. Werkmeister S, Dawson A, Wellner F (2004) Pavement design model for unbound granular materials. Journal of Transportation Engineering 130(5):665-674.

39. Yang L, Powrie W, Priest J (2009) Dynamic stress analysis of a ballasted railway track bed during train passage. Journal of Geotechnical and Geoenvironmental Engineering 135(5):680–689.

List of Tables

Table 1: Test program

List of Figures

Fig. 1: Grain size distribution of the studied materials
Fig. 2: Deviator stress versus axial strain for test ITL_5w6 - Determination of resilient modulus
Fig. 3: Deviator stress versus axial strain for test ITL_5w6. a) N = 1-8 (Δq_{max} = 45 kPa); b) from Δq_{max} = 45 kPa (N = 30 000) to Δq_{max} = 90 kPa (N = 30 001 - 30 0004); c) from Δq_{max} = 90 kPa (N = 60 000) to Δq_{max} = 145 kPa (N = 60 001 - 60 0004); d) from Δq_{max} = 145 kPa (N = 90 000) to Δq_{max} =20 kPa (N = 90 001 - 90 0004)
Fig. 4: Resilient strain versus number of cycles in test $ITL_{10}w12$
Fig. 5: Resilient modulus versus number of cycles for ITL_{10}. a) *w* = 4%; b) *w* = 6%; c) *w* = 12%
Fig. 6: Resilient modulus versus number of cycles for ITL_5w6
Fig. 7: Resilient modulus versus number of cycles for ITL_0. a) *w* = 4%; b) *w* = 6%; c) *w* = 12%
Fig. 8: Resilient modulus versus number of cycles for ITL_{-10}. a) *w* = 4%; b) *w* = 6%; c) *w* = 12%
Fig. 9: End-stage resilient modulus versus deviator stress - Effect of water content. a) ITL_{10}; b) ITL_0; c) ITL_{-10}
Fig. 10: End-stage resilient modulus versus deviator stress - Effect of fines content. a) *w* = 4%; b) *w* = 6% and c) *w* = 12%
Figure 11: Resilient modulus in function of water content at different fine contents; a) at Δq_{max} = 45 kPa and b) at Δq_{max} = 140 kPa

Table 1: Test program

Soil	Water content - *w* (%)		
	4 %	6 %	12 %
ITL_{10}	$ITL_{10}w4$	$ITL_{10}w6$	$ITL_{10}w12$
ITL_{5}	-	$ITL_{5}w6$	-
ITL_{0}	$ITL_{0}w4$	$ITL_{0}w6$	$ITL_{0}w12$
ITL_{-10}	$ITL_{-10}w4$	$ITL_{-10}w6$	$ITL_{-10}w12$

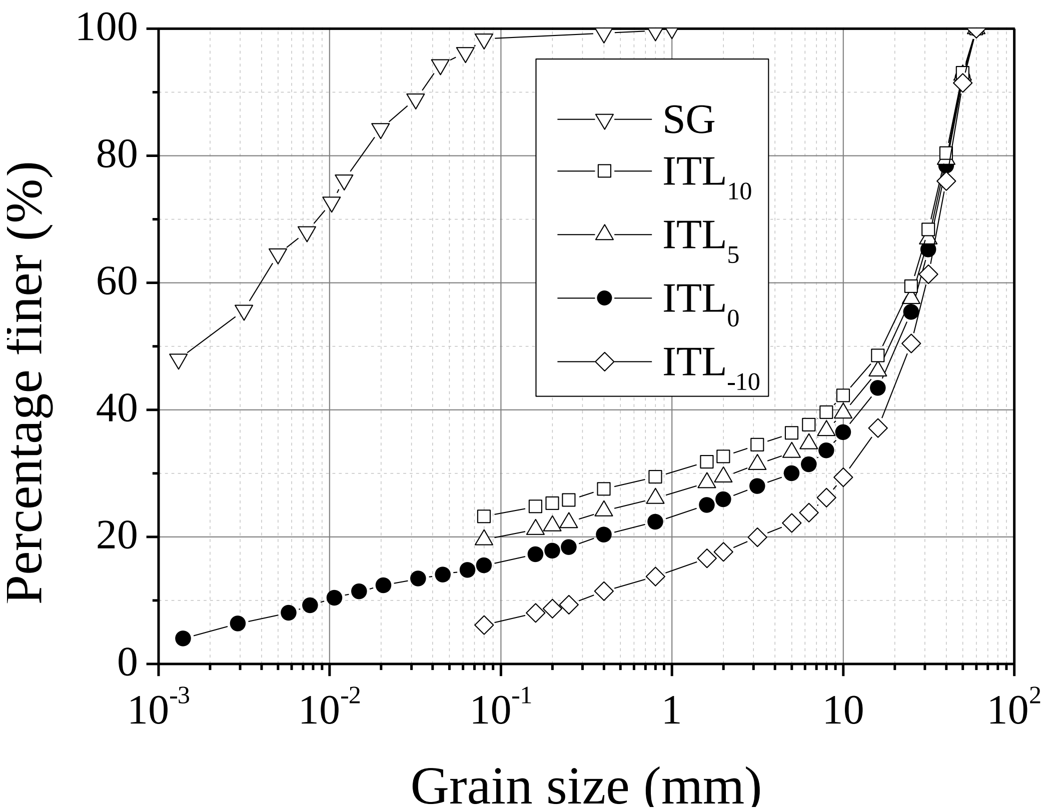

Fig. 1: Grain size distribution of the studied materials

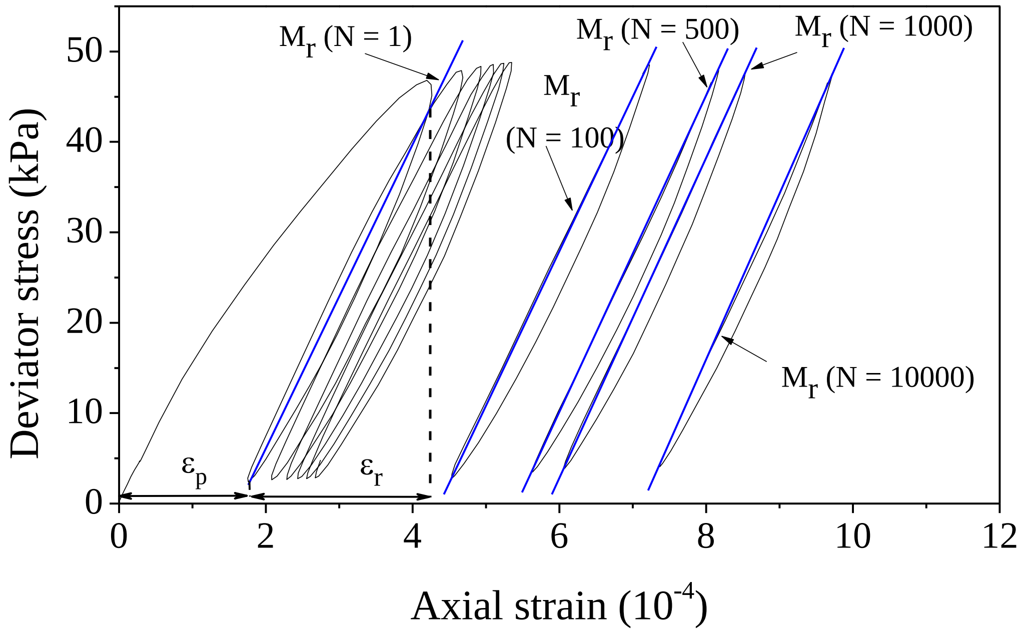

Fig. 2: Deviator stress versus axial strain for test ITL$_5$w6 - Determination of resilient modulus

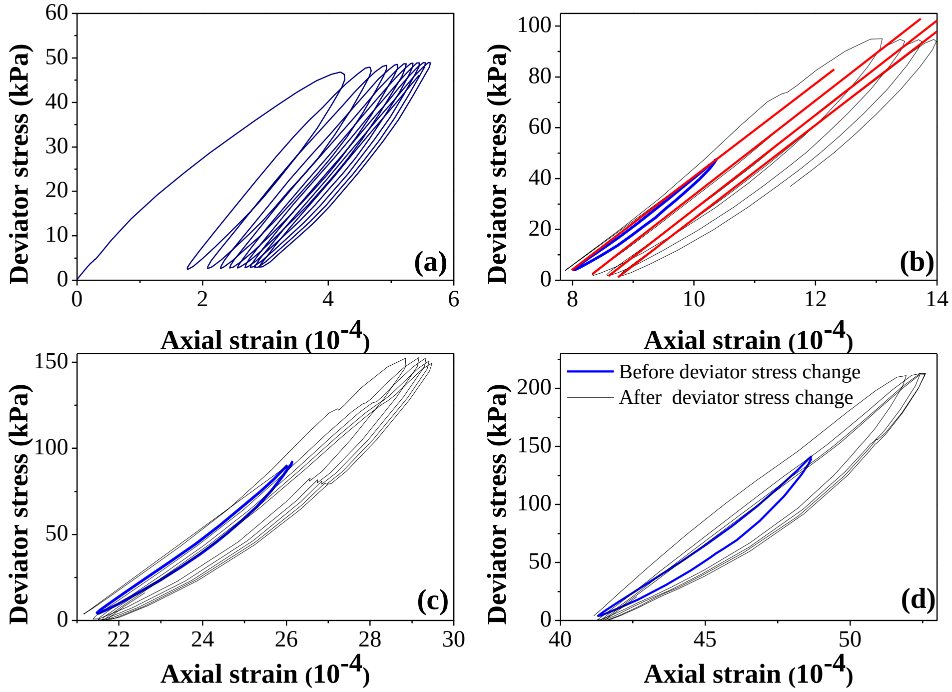

Fig. 3: Deviator stress versus axial strain for test ITL$_5$w6. a) N = 1-8 (Δq_{max} = 45 kPa); b) from Δq_{max} = 45 kPa (N = 30 000) to Δq_{max} = 90 kPa (N = 30 001 - 30 0004); c) from Δq_{max} = 90 kPa (N = 60 000) to Δq_{max} = 145 kPa (N = 60 001 - 60 0004); d) from Δq_{max} = 145 kPa (N = 90 000) to Δq_{max} =20 kPa (N = 90 001 - 90 0004)

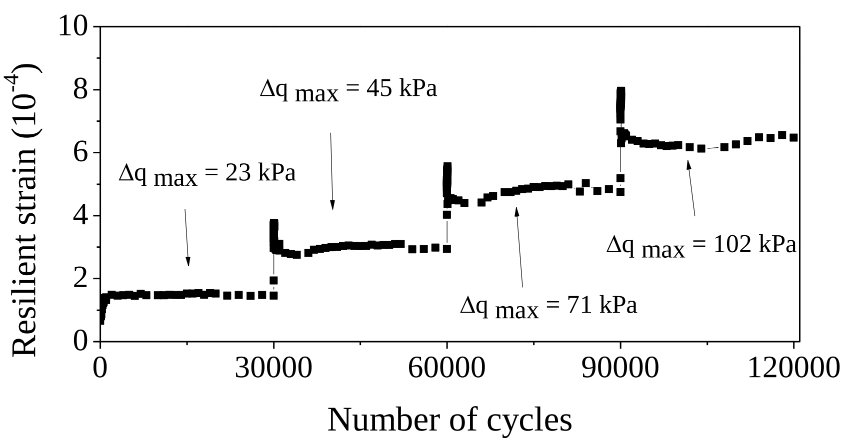

Fig. 4: Resilient strain versus number of cycles in test ITL$_{10}$w12

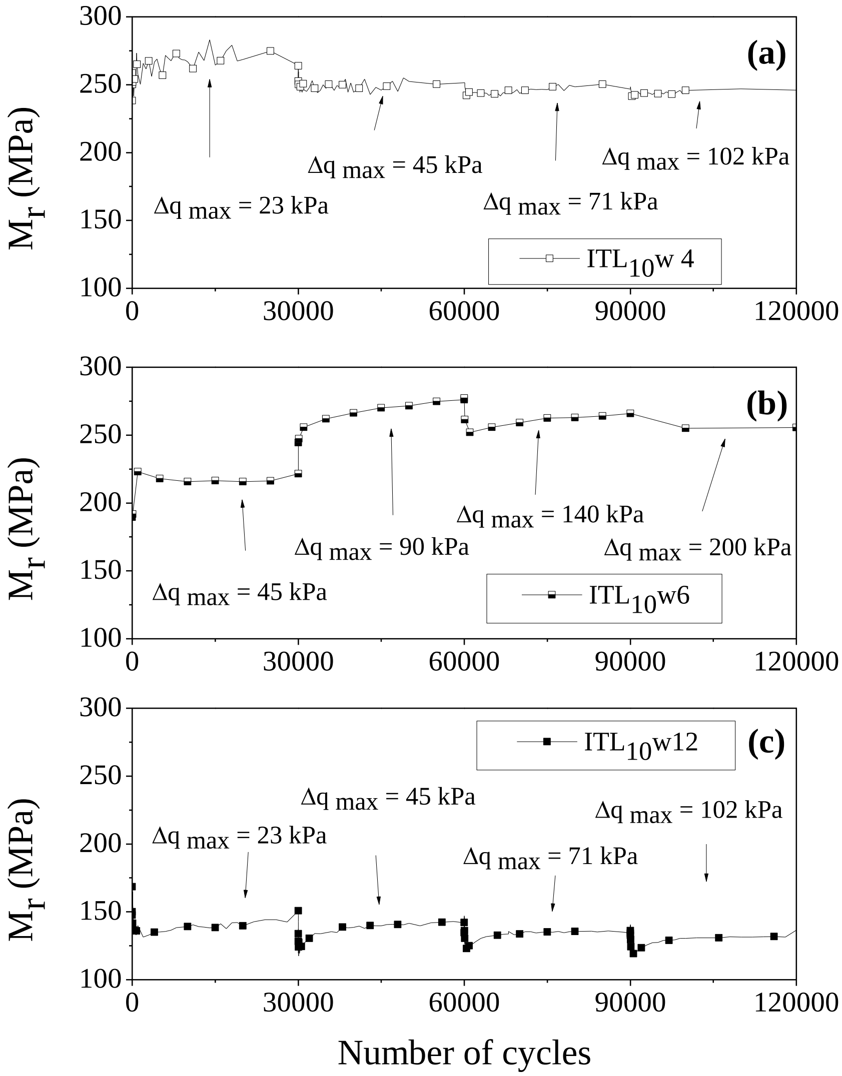

Fig. 5: Resilient modulus versus number of cycles for ITL_{10}. a) *w* = 4%; b) *w* = 6%; c) *w* = 12%

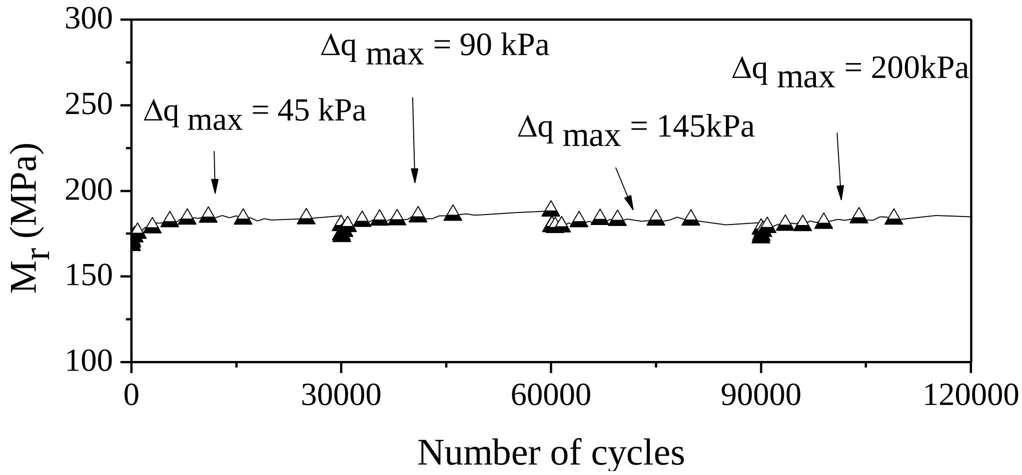

Fig. 6: Resilient modulus versus number of cycles for ITL_5w6

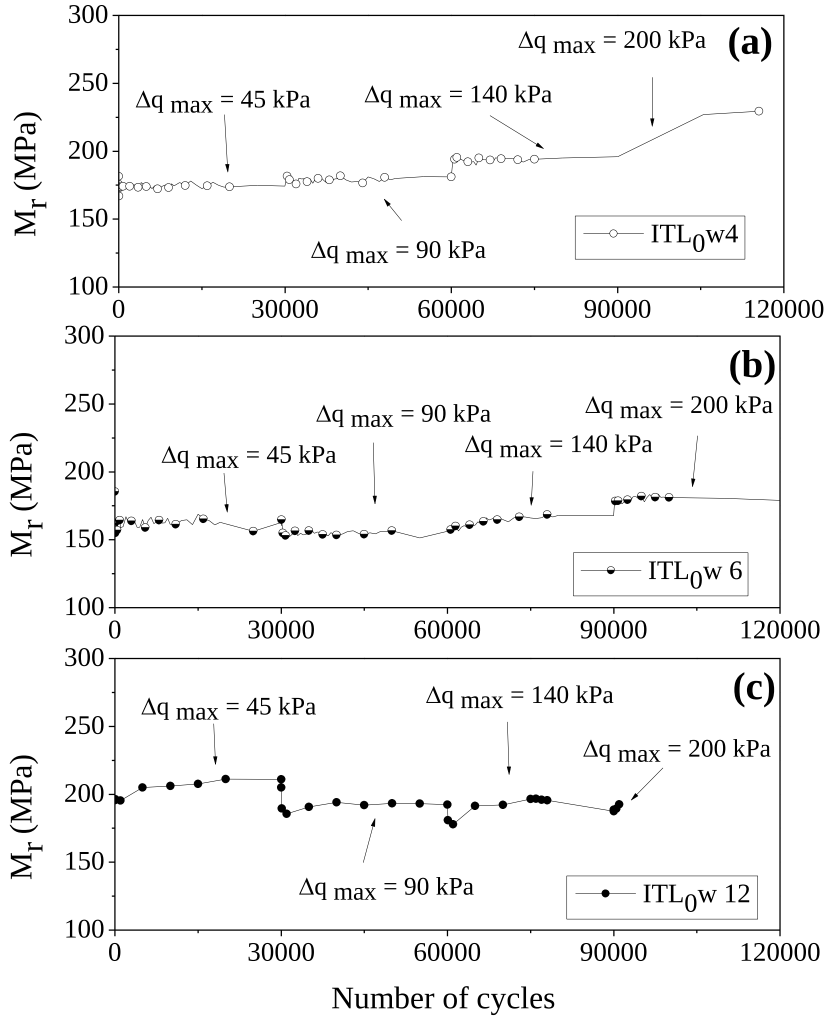

Fig. 7: Resilient modulus versus number of cycles for ITL$_0$. a) *w* = 4%; b) *w* = 6%; c) *w* = 12%

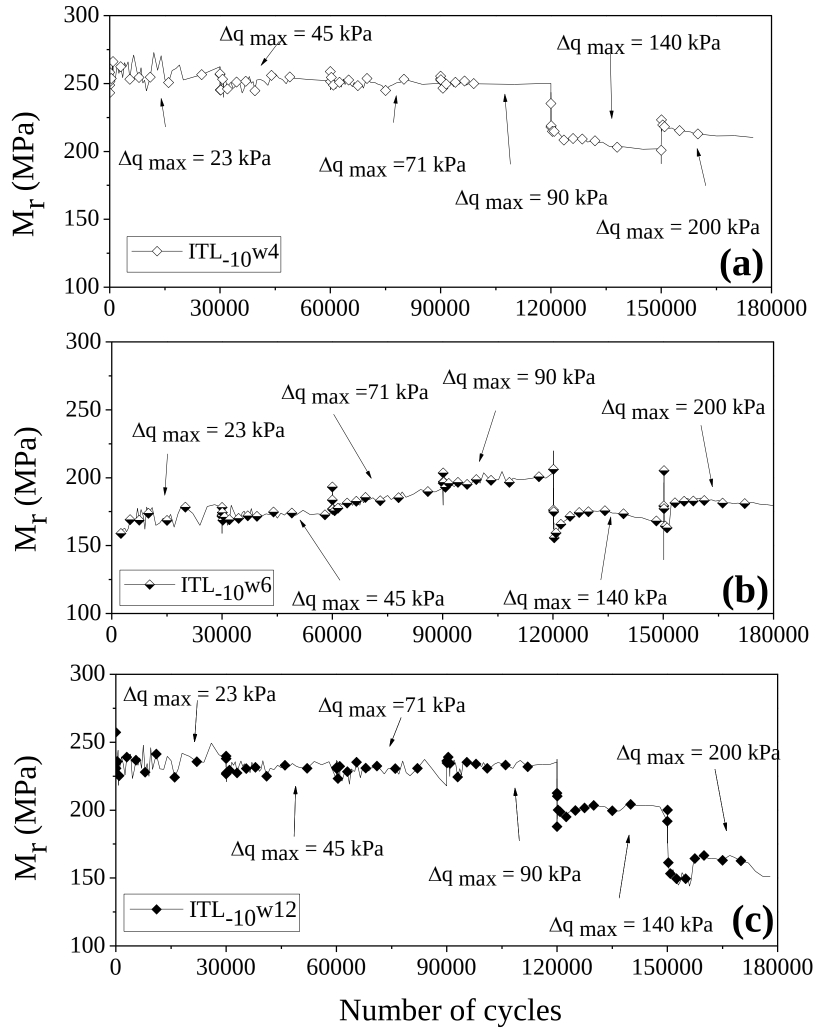

Fig. 8: Resilient modulus versus number of cycles for ITL$_{-10}$. a) *w* = 4%; b) *w* = 6%; c) *w* = 12%

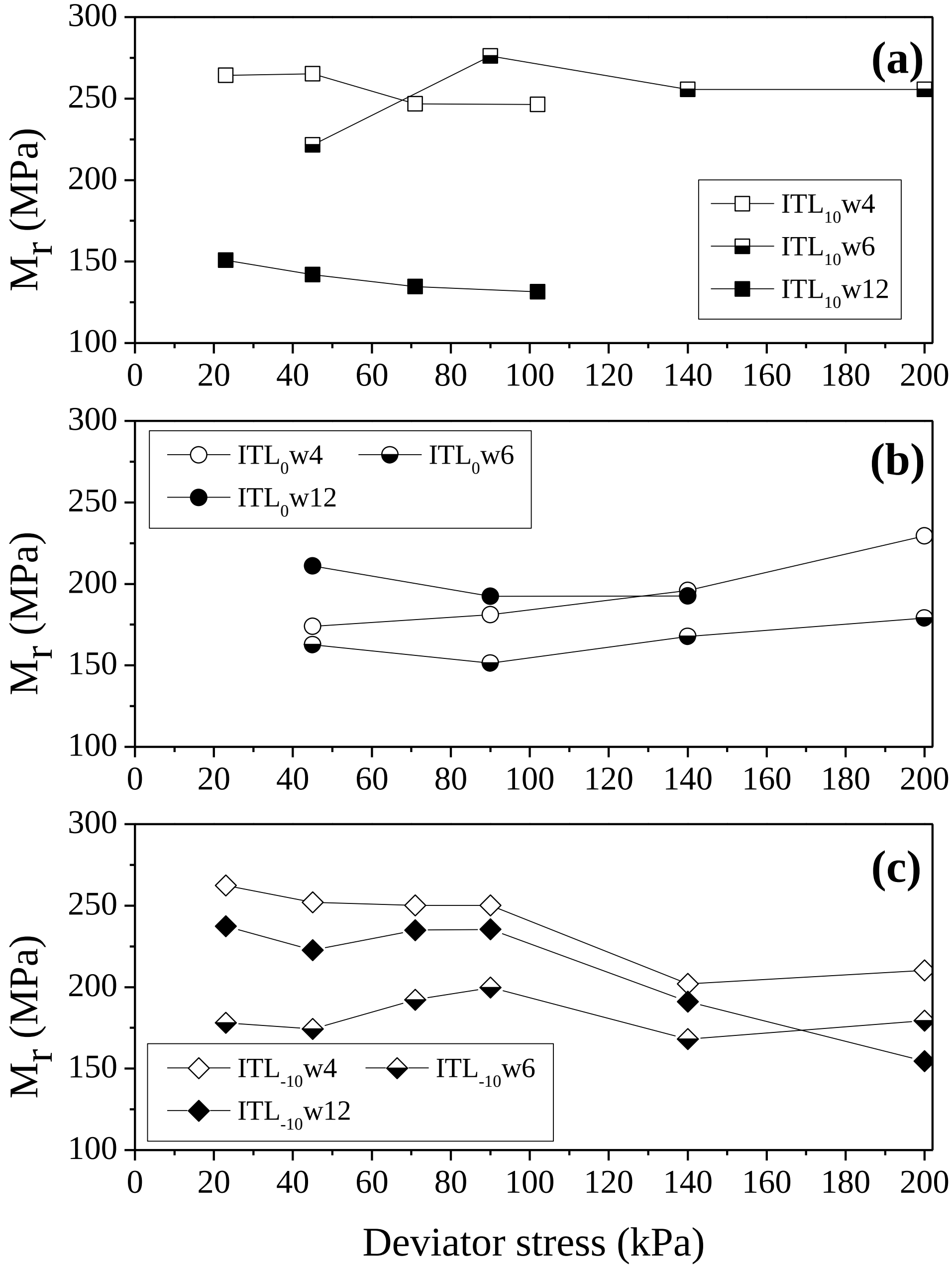

Fig. 9: End-stage resilient modulus versus deviator stress - Effect of water content. a) $\boldsymbol{ITL_{10}}$; b) $\boldsymbol{ITL_{0}}$; c) $\boldsymbol{ITL_{-10}}$

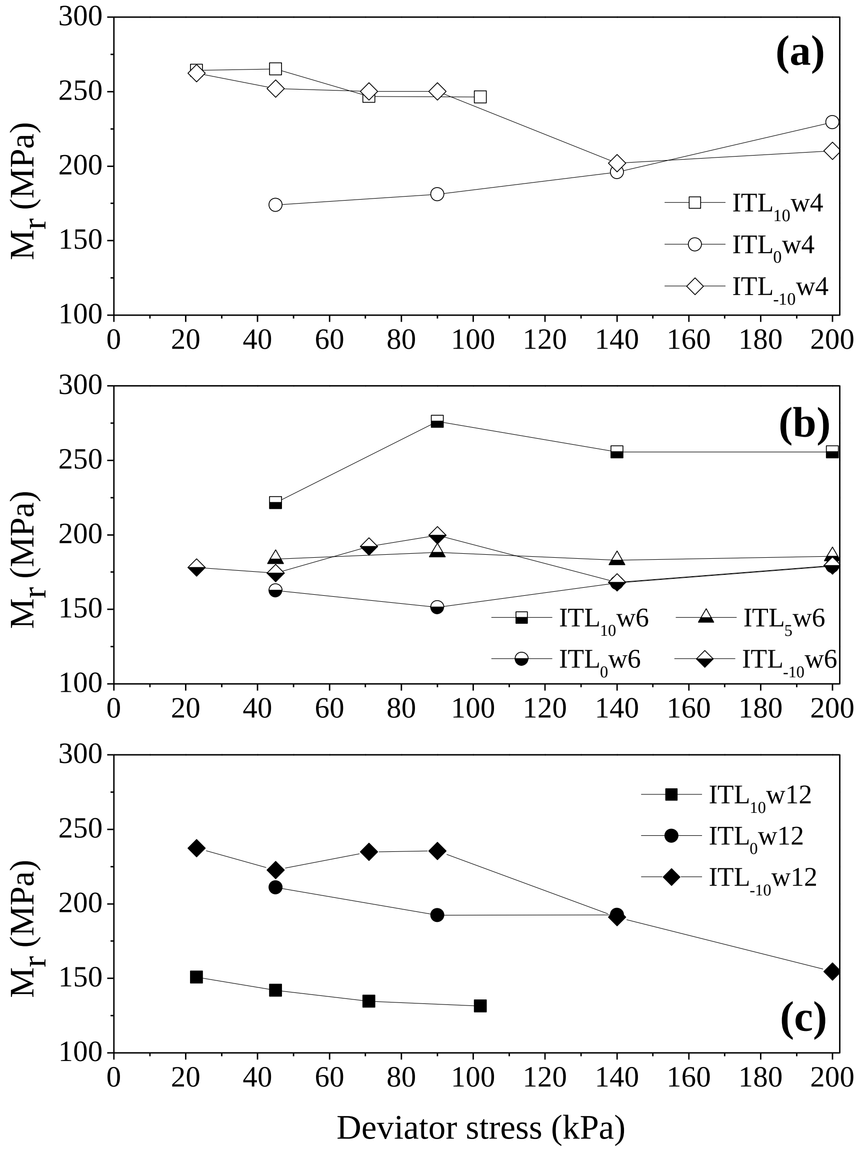

Fig. 10: End-stage resilient modulus versus deviator stress - Effect of fines content. a) *w* = 4%; b) *w* = 6% and c) *w* = 12%

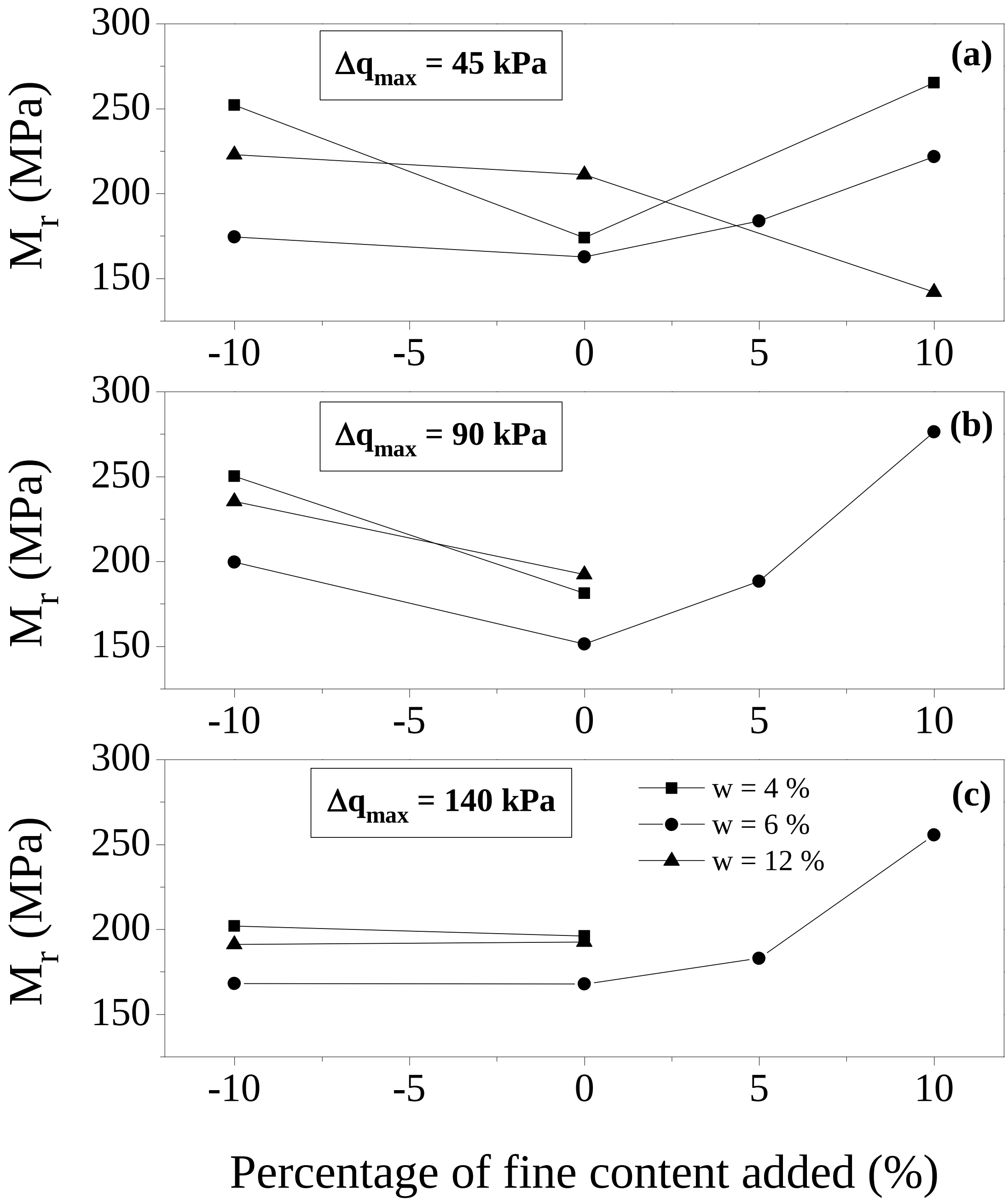

Figure 11: Resilient modulus in function of water content at different fine contents; a) at Δq_{max} = 45 kPa; b) at Δq_{max} = 90 kPa and c) at Δq_{max} = 140 kPa